Eur. Phys. J. B **9**, 215–223 (1999)

THE EUROPEAN PHYSICAL JOURNAL B
EDP Sciences

Numerical diagonalization analysis of the ground-state superfluid-localization transition in two dimensions

Y. Nishiyama[a]

Department of Physics, Faculty of Science, Okayama University, Okayama 700-8530, Japan

Received 19 August 1998

Abstract. Ground state of the two-dimensional hard-core-boson system in the presence of the quenched random chemical potential is investigated by means of the exact-diagonalization method for the system sizes up to $L = 5$. The criticality and the DC conductivity at the superfluid-localization transition have been controversial so far. We estimate, with the finite-size scaling analysis, the correlation-length and the dynamical critical exponents as $\nu = 2.3 \pm 0.6$ and $z = 2$, respectively. The AC conductivity is computed with the Gagliano-Balseiro formula, with which the resolvent (dynamical response function) is expressed in terms of the continued-fraction form consisting of Lanczos tri-diagonal elements. Thereby, we estimate the universal DC conductivity as $\sigma_c(\omega \to 0) = 0.135 \pm 0.01((2e)^2/h)$.

PACS. 75.10.Jm Quantized spin models – 75.10.Nr Spin-glass and other random models – 75.40.Mg Numerical simulation studies

1 Introduction

The scaling argument of Abrahams, Anderson, Licciardello and Ramakrishnan [1] states that in *two* dimensions, infinitesimal amount of quenched randomness should drive itinerant extended states to localize. That is, at the absolute zero temperature, the conductivity should be vanishing, if there exist any randomnesses. These are, however, some exceptions where the above description fails. For instance, the integer quantum hall effect is described in terms of *successive* metal-insulator (delocalization-localization) transitions of dirty two-dimensional electron system with the external magnetic field varied. In the above-mentioned scaling theory, the random perturbation is appeared to be marginal so that some unexpected factors, namely, the magnetic field and the many-body interaction, would possibly change the scenario.

For instance, suppose that there exists an attractive interaction among the electrons. At the ground state, the electrons would be unstable against the bose condensation so that the system would be in the superconducting phase. The disorder-driven localization from the superconducting phase is apparently out of the scope of the conventional localization theory, and has been studied extensively so far. In experiments, the transition is observed for metallic films [2–5], high-T_c films [6] and Josephson-junction arrays [7,8]. One of the main concerns is the conductivity at the critical point: the experiments show that irrespective of the samples examined, the localization transition occurs at a universal condition. Namely, at the transition, the electrical conductivity is found to be $\approx (2e)^2/h$ (the parameter e denotes the charge of a single electron, and h denotes the Planck constant).

Localization transition of the absorbed helium by a porous media [9,10] is considered [11,12] to belong precisely to the same universality class mentioned above. (That is, the critical exponents are identical. The electrical conductivity, however, does not make any sense for the latter, because the helium atom is not charged.) The equivalence is based on the belief that the Cooper pair is formed already in the localization phase as well as in the superconducting phase, and the essence of the transition is concerned only in the boson degrees of freedom and the site-random chemical potential. This picture was found to be valid in one dimension [13].

From a theoretical viewpoint, the criticality itself is a matter of interest. It is notable that the present phenomenon occurs at the ground state. This criticality is different essentially from that of the finite-temperature transitions. In the path-integral picture for the partition function, d-dimensional quantum system is regarded as a $(d+1)$-dimensional classical system. The system-size along the imaginal-time direction is given by the inverse temperature, which is diverging at the ground state. Hence, the critical fluctuation along the imaginary-time direction contributes to the universality class significantly. This extra contribution is characterized by the dynamical critical exponent z, which is explained in the next section in detail.

The scaling argument [12,14] shows that the conductivity remains finite at the onset of the localization transition even at the ground state. Moreover, the argument

[a] e-mail: kitarou@soroban.phys.okayama-u.ac.jp

for general dimensions yields the dynamical critical exponent being equal to the spatial dimension; $z = d$. We explain the argument in Section 2.2. This prediction is astonishing in the sense that there is no upper critical dimension in this critical phenomenon. (The prediction is confirmed rigorously for $d = 1$, where the bosonization technique is available [13,15]. For numerical study of the $d = 1$ criticality, see the article [16] and references therein.) Because of the absence of the upper critical dimension, the ϵ-expansion scheme cannot be formulated. Hence, for $d = 2$, numerical-simulation studies have been playing a crucial role so far.

Runge [17] employed the exact-diagonalization method to treat system sizes up to $L = 4$; the Hamiltonian is given by equation (1) shown afterwards. (When treating $L = 5$, he reduced the particle density to $n = 0.2$.) He obtained the estimates $\nu = 1.4 \pm 0.3$, $z = 1.95 \pm 0.25$ and $\sigma_{\rm c} = 0.17 \pm 0.01((2e)^2/h)$, and claimed that finite-size correction prevents definite conclusion. Monte-Carlo method has been used in many studies. Makivić, Trivedi and Ullah [18] obtained the estimates $\nu = 2.2 \pm 0.2$, $z = 0.5 \pm 0.05$ and $\sigma_{\rm c} = 1.2 \pm 0.2$. Batrouni, Larson, Scalettar, Tobochnik and Wang [19] obtained the estimate $\sigma_{\rm c} = 0.45 \pm 0.07$. Wallin, Sørensen, Girvin and Young [20] obtained $\nu = 0.9 \pm 0.1$, $z = 2.0 \pm 0.1$ and $\sigma_{\rm c} = 0.14 \pm 0.03$. Sørensen, Wallin, Girvin and Young [21] obtained $\nu = 1.0 \pm 0.1$, $z = 2.0 \pm 0.1$ and $\sigma = 0.14 \pm 0.03$. Zhang, Kawashima, Carlson and Gubernatis [22] obtained $\nu = 0.9 \pm 0.1$ and $z = 2.0 \pm 0.4$. The estimates are still rather scattering. In particular, computing the conductivity more reliably would be of practical importance, because it can be compared with the experimentally observed value $\sigma_{\rm c} \approx (2e)^2/h$ mentioned above. The Monte-Carlo method enables one to treat larger systems than those with the exact-diagonalization method. rather than In the quantum Monte-Carlo simulation, however, because the dynamical critical exponent is predicted to be $z = 2$, in order to simulate ground-state property, the imaginary-time system size should be enlarged *rapidly*; namely, it should be kept quadratic in terms of the real-space system size at least.

In the present paper, we simulate the two-dimensional bose system on the $L \times L$ square lattice under the periodic boundary condition in the presence of the quenched random chemical potential. The Hamiltonian is given by,

$$\mathcal{H} = -\frac{J}{2} \sum_{\langle ij \rangle} \left(a_i^\dagger a_j + \text{h.c.} \right) + \sum_i H_i (2 a_i^\dagger a_i - 1), \qquad (1)$$

where the operators $\{a_i, a_i^\dagger\}$ obey the hard-core boson statistics,

$$[a_i, a_j] = [a_i^\dagger, a_j^\dagger] = [a_i, a_j^\dagger] = 0 \quad (i \neq j),$$
$$\{a_i, a_i^\dagger\} = 1 \quad \text{and} \quad a_i a_i = a_i^\dagger a_i^\dagger = 0, \qquad (2)$$

and $\sum_{\langle ij \rangle}$ denotes the summation over all nearest neighbors. The site-random chemical potentials $\{H_i\}$ distribute uniformly over the range $[-\sqrt{3}\Delta, \sqrt{3}\Delta]$; namely, the mean deviation is given by $\sqrt{[H_i^2]_{\rm av}} = \Delta$. The particle density $n = N/L^2$ is fixed to be one half throughout this paper.

As is mentioned above, the model (1) is believed to describe the physics of the superconductivity-localization transition as well as the superfluid-localization transition. This belief is based on the picture [11,12] that the boson describes the Cooper pair, so that the boson charge should be the twice of the single electron charge; $e^* = 2e$. The model (1) is investigated very extensively in the above mentioned article [17]. Here, we attempt to improve this work through utilizing some recent developments, the algorithm for computing the response function (resolvent) [23], the estimate scheme of the dynamical critical exponent [24], and parallel supercomputers which enable one to treat larger system ($L = 5$). These improvements are described in respective subsections of Section 3.

The rest of the paper is organized as follows: in the next section, we review some notions relevant to the present study. First, we show the viewpoint from which the model (1) is regarded as the quantum XY model [25]. Nature of the superfluid-localization transition is interpreted in the language of the quantum spin system. Then, we summarize the scaling argument [12,14] describing the criticality. The argument yields some scaling formulae which are useful in analyzing our finite-size numerical data. In Section 3, our numerical simulation results are presented. We estimated the critical exponents as $\nu = 2.3 \pm 0.6$ and $z = 2$. At the critical point, we estimate the conductivity as $\sigma_{\rm c} = 0.135 \pm 0.01((2e)^2/h)$. These new results are summarized in the last section in comparison with previous results.

2 Review – Equivalence to the XY model and scaling argument

In this section, we summarize several important aspects about the model (1). First, we introduce the equivalence between the model (1) and the quantum XY spin system [25]. This equivalence reveals nature of both the superfluid and the localization phases in the language of the spin system, and provides intuitive picture of the phase transition. Finally, we review the scaling argument [12, 14], whose formulae are used in the analyses of our numerical data in Section 3.

2.1 Mapping to the quantum XY model with the random magnetic field

Because the $S = 1/2$ ladder operators $\{S_i^+, S_i^-\}$ obey the same algebra equations (2) [25], the Hamiltonian (1) is expressed in terms of the spin operators,

$$\mathcal{H} = -J \sum_{\langle ij \rangle} (S_i^x S_j^x + S_i^y S_j^y) + 2 \sum_i H_i S_i^z. \qquad (3)$$

Now, perspectives developed for the quantum spin system become available. Kishi and Kubo [26] showed rigorously

that (without the random magnetic field) in the thermodynamic limit, the ground-state magnetism is spontaneously broken

$$\langle \mathbf{m}_{XY}^2 \rangle \neq 0, \tag{4}$$

where $\mathbf{m}_{XY} = \frac{1}{L^2}\sum_i (S_i^x, S_i^y)$. It is expected that for sufficiently strong random fields, the long-range magnetism would be disturbed, $\langle \mathbf{m}_{XY}^2 \rangle = 0$. Hence, we see that a phase transition between the XY and the random-field phases would exist at a certain random-field strength.

What does the existence of the XY order (4) stand for in the boson language? We show that it stands for the bose condensation (superfluidity): if the number of the particles condensing at the $\mathbf{k} = 0$ state is of the system-size order, the state is regarded as being of superfluid. That is, the quantity,

$$|\Psi_{\rm super}|^2 = \frac{1}{L^2}\left\langle \left(\frac{1}{L}\sum_{\mathbf{j}} \mathrm{e}^{\mathrm{i}\mathbf{k}\cdot\mathbf{j}} a_{\mathbf{j}}^\dagger\right)\left(\frac{1}{L}\sum_{\mathbf{j}} \mathrm{e}^{-\mathrm{i}\mathbf{k}\cdot\mathbf{j}} a_{\mathbf{j}}\right)\right\rangle\Bigg|_{\mathbf{k}=\mathbf{0}}, \tag{5}$$

works as an order parameter of the superfluidity. The order parameter is expressed in term of the spin language, $|\Psi_{\rm super}|^2 = \langle \mathbf{m}_{XY}^2 \rangle$. As is explained above, this remains finite. And so, the superfluidity develops actually at the ground state of the Hamiltonian (1) at $\Delta = 0$. It is quite natural that the gauge degree of freedom, which is spontaneously broken in the superfluid phase, is related to the in-plain spin rotator. As is introduced in Section 1, the essence of the superfluid-localization transition is believed to be concerned only in the in-plain rotator degrees of freedom, and the site-random perturbations conjugate to them.

2.2 Scaling argument

Here, we introduce a scaling argument [12,14] which describes the criticality of the superfluid-localization transition. The argument yields various useful formulae to analyze numerical data. The argument itself, however, does not yield any conclusions to estimate the critical exponents quantitatively. Any analytical analyses to estimate the critical exponents face a difficulty as is mentioned in Introduction. For the purpose of estimating the exponents quantitatively, numerical simulation has been playing a crucial role.

The scaling hypothesis states that (the singular part of) the free energy per unit volume for the system size L and the inverse temperature β should be given in the form,

$$f(L,\beta) \sim \frac{1}{\xi_{\rm r}^d \xi_\tau} \tilde{f}\left(\frac{L}{\xi_{\rm r}}, \frac{\beta}{\xi_\tau}\right), \tag{6}$$

where $\xi_{\rm r}$ and ξ_τ denote the real-space correlation length and the imaginary-time one, respectively. (Note that in the path-integral viewpoint, the partition function of a d-dimensional quantum system is regarded as that of a $(d+1)$-dimensional counterpart.) These are expressed in term of the deviation from the critical point δ; $\xi_{\rm r} \sim \delta^{-\nu}$ and $\xi_\tau \sim \xi_{\rm r}^z$. The parameter ν denotes the correlation-length critical exponent, and z denotes the dynamical critical exponent. These are estimated in Section 3, numerically. In general, for quantum random systems, the real-space correlation develops less robustly than the imaginary-time one does. This anisotropy is one of the significant characteristics of the random quantum critical phenomena, resulting in various new exotic universality classes. The anisotropy is characterized by the dynamical critical exponent z.

The superfluid density $\rho_{\rm s}$ – the spin stiffness in the language of the spin system – is defined as the elastic constant in terms of the real-space gauge twist [27],

$$f \sim \frac{\rho_{\rm s}}{2}(\partial_x \theta)^2. \tag{7}$$

Note that the quantity works as an order parameter of the superfluidity. It is furthermore expressed in the form, $f \sim \frac{\rho_{\rm s}}{2}\left(\frac{\Theta}{L}\right)^2$, where Θ denotes the total gauge twist. Using the form (6), we obtain,

$$\begin{aligned}\rho_{\rm s} \sim fL^2 &= \xi_{\rm r}^{-(d+z-2)} \tilde{\tilde{f}}\left(\frac{L}{\xi_{\rm r}}, \frac{\beta}{\xi_\tau}\right) \\ &= L^{-(d+z-2)} \tilde{\tilde{f}}\left(\frac{L}{\xi_{\rm r}}, \frac{\beta}{\xi_\tau}\right).\end{aligned} \tag{8}$$

This scaling form is used in our numerical-data analysis. The compressibility κ is defined, on the other hand, as the elastic constant of the imaginary-time gauge twist, $f \sim \frac{\kappa}{2}(\partial_\tau \theta)^2$. Through the similar arguments as the above, we obtain the scaling formula for the compressibility,

$$\kappa \sim \xi_{\rm r}^{-(d-z)} \tilde{\tilde{f}}\left(\frac{L}{\xi_{\rm r}}, \frac{\beta}{\xi_\tau}\right). \tag{9}$$

Fisher, Weichman, Grinstein and Fisher predicted that the formula,

$$z = d, \tag{10}$$

should hold for any dimensions: the compressibility is finite in both phases beside the transition point. Hence, it would be kept to be of the order unity even at the critical point as well, so that we obtain the equality (10). In Section 3, we confirm their prediction with use of the Rieger-Young method [24].

Finally, we explain how the above scaling argument concludes that the conductivity would be finite at the critical point. The scaling argument [14] yields the following formula for the AC conductivity,

$$\sigma(\omega) \sim \xi_{\rm r}^{-(d+z-2)} \tilde{\tilde{\rho}}_{\rm s}(\omega\xi_\tau)/\omega. \tag{11}$$

Assuming $d = 2$, and the scaling function behaves as $\tilde{\tilde{\rho}}_{\rm s}(x) \propto x$ in the vicinity of the critical point $x \to \infty$, we see that the conductivity does not have any singularities at the critical point, and therefore remains *finite*. To summarize, the scaling argument states that there is a possibility that the conductivity remains finite at the superfluid-localization critical point. The quantitative evaluation of

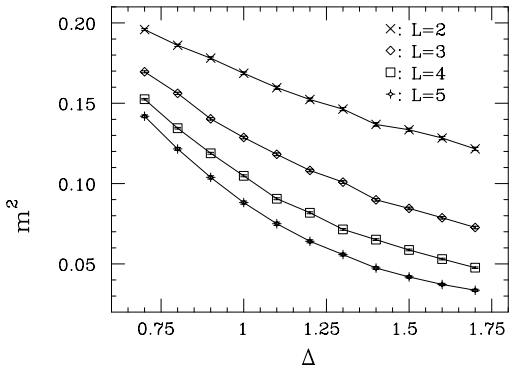

Fig. 1. Square of the in-plain magnetization m^2 is plotted against the randomness Δ. The random-sample numbers are 2048, 2048, 2048 and 608 for $L = 2$, 3, 4 and 5, respectively. The XY magnetic order becomes suppressed as the random magnetic field is strengthened.

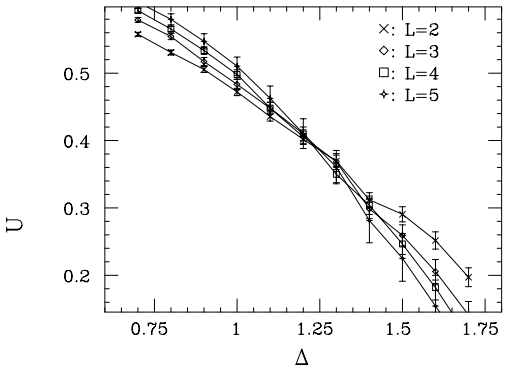

Fig. 2. Binder parameter (12) of the in-plain magnetization is plotted against the randomness. The intersection point of the curves indicates the location of the transition point.

$\sigma_{\rm c}$, however, lies out of the scope of the argument. Here, we compute the conductivity with use of the Gagliano-Balseiro method [23] in the next section.

3 Numerical results

In this section, we present our numerical results. In order to diagonalize the Hamiltonian (1), we employed the Lanczos method. We have fixed the particle density to be one half $n\,(=N/L^2) = 0.5$, and treated the system sizes up to $L = 5$. For those system sizes of odd L, we proceeded the sets of simulations for the particle numbers $N = [L^2/2]$ and $[L^2/2] - 1$; the bracket $[\cdots]$ denotes the Gauss notation. The data for $n = 0.5$ are obtained through interpolating these two sets of data with use of the relation $Q(n) = a(n - 0.5)^2 + c$; physics is symmetric in terms of $n = 0.5$ (particle-hole symmetry).

3.1 Criticality of the superfluid-localization transition

Here, we determine the location of the superfluid-localization transition point and the correlation-length critical exponent. We use the language of the spin system, which is explained in the Section 2.1. That is, from this viewpoint, the transition is characterized by the disappearance of the XY (in-plain) magnetic order.

In Figure 1, we plotted the square of the in-plane magnetization $m^2 = [\langle \mathbf{m}_{XY}^2 \rangle]_{\rm av}$ against the randomness, where the bracket $[\cdots]_{\rm av}$ denotes the random-sampling average, and $\langle \cdots \rangle$ denotes the ground-state expectation value. The random-sample numbers are 2048, 2048 2048 and 608 for $L = 2$, 3, 4 and 5, respectively. We see that the in-plane magnetization becomes suppressed by the randomness. In Figure 2, we plotted the Binder parameter [28] of the in-plane magnetic order,

$$U = 1 - \frac{[\langle \mathbf{m}_{XY}^4 \rangle]_{\rm av}}{3[\langle \mathbf{m}_{XY}^2 \rangle^2]_{\rm av}} \cdot \tag{12}$$

The Binder parameter is invariant with respect to the system sizes at the critical point. It is enhanced (suppressed) in the order (disorder) region as the systems size is enlarged. In Figure 2, We observe an intersection point at $\Delta \approx 1.2$. Namely, in the region $\Delta < 1.2$, the superfluidity persists against the random chemical potential, whereas in $\Delta > 1.2$, the particles are localized, and the long-range gauge coherence is lost.

In order to estimate the transition point and the correlation-length exponent precisely, we analyze the above data by means of the finite-size-scaling theory. According to the theory, the Binder parameter (dimensionless quantity) obeys the form $U = \tilde{U}\left((\Delta - \Delta_{\rm c})L^{1/\nu}\right)$ in the vicinity of the critical point $\Delta_{\rm c}$. Namely, the data $(\Delta - \Delta_{\rm c})L^{1/\nu}$-$U$ should collapse along a universal curve irrespective of the system sizes. In other words, the critical point $\Delta_{\rm c}$ and the exponent ν are adjusted so that the scaled data could form a universal curve. The degree to what extent the data collapse is measured by the Kawashima-Ito "local-linearity function" [29] which is explained in Appendix. In Figure 3, we show the scaling plot for the data shown in Figure 2. In consequence, we obtain the estimates $\Delta_{\rm c} = 1.25 \pm 0.1$ and $\nu = 2.3 \pm 0.6$. In order to see whether the correction to the finite-size scaling exists, we analyzed the data for $L = 3$, 4 and 5 similarly; omitted the data for $L = 2$. This analysis yields the best-fit estimates $\Delta_{\rm c} = 1.27$ and $\nu = 2.3$. Therefore, we conclude that there is little correction to the finite-size scaling; in other words, the system sizes treated here reach the scaling region. Our estimate $\nu = 2.3 \pm 0.6$ is somewhat different from that of reference [17] ($\nu = 1.4 \pm 0.3$) despite of the fact that we considered the same model also using the exact-diagonalization technique. This discrepancy may originate in the criteria utilized to appreciate the scaling-data collapse, and is discussed in the next section.

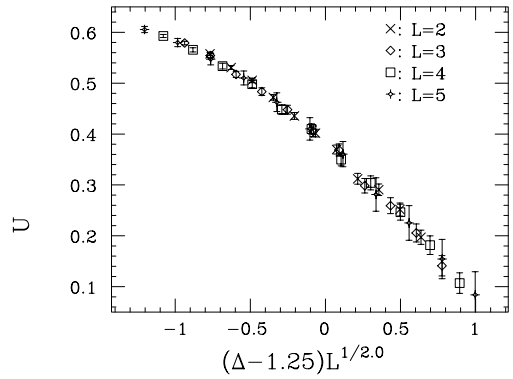

Fig. 3. Scaling plot for the data shown in Figure 2. The scaling analysis yields the best-fit estimates $\Delta_{\rm c} = 1.25$ and $\nu = 2.0$.

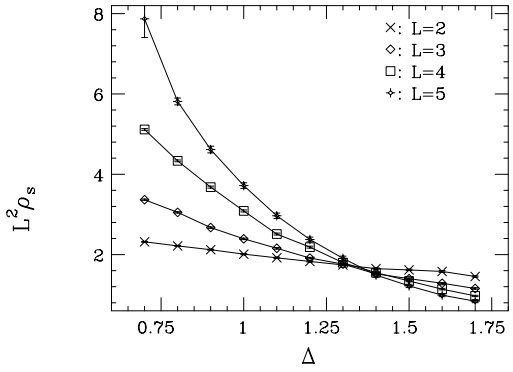

Fig. 4. Scaled spin stiffness $L^2\rho_{\rm s}$ is plotted. Because the curves intersect at a point, the prediction $z = d$ is appeared to hold.

According to the formula (8), if we assume that the dynamical critical exponent is equal to the spatial dimension, namely, $z = d = 2$, the scaled spin stiffness $L^2\rho_{\rm s}$ should be invariant at the critical point. The spin stiffness is given by,

$$\rho_{\rm s} = \left[\left\langle \frac{\partial^2 E_{\rm g}(\Theta)}{\partial \Theta^2} \bigg|_{\Theta=0} \right\rangle \right]_{\rm av} , \qquad (13)$$

where the angle denotes the boundary gauge twist $a_i^\dagger a_j \to {\rm e}^{{\rm i}\Theta} a_i^\dagger a_j$, and $E_{\rm g}$ denotes the ground-state energy. In Figure 4, we plotted the scaled spin stiffness $L^2\rho_{\rm s}$. In fact, we observe at $\Delta \approx 1.3$, all the curves intersect. In consequence, founded on the scaling formula (8), the so-called "generalized Josephson relation", we see that the dynamical exponent would be equal to two. The same reasoning founded on this relation has been reported in the literatures [17,18,20,22]. In this paper, in Section 3.3, we estimate the dynamical critical exponent with use of the Rieger-Young [24] method, which would be more straightforward.

3.2 Electrical conductivity

We evaluate the dynamical conductivity at the critical point $\Delta_{\rm c} = 1.25$ estimated in the above section. The DC conductivity is conjectured to be universal at the critical point as is explained in Introduction. The dynamical conductivity is given by the current-current time correlation,

$$\sigma(\omega) = {\rm Re} \left[\frac{1}{\hbar\omega} \frac{1}{L^2} \int_0^\infty {\rm d}t {\rm e}^{{\rm i}\omega t} \langle [J_x(t), J_x] \rangle \right]_{\rm av} , \qquad (14)$$

where the current is given by $J_x = \frac{{\rm i}e^* J}{2\hbar} \sum_{j,\delta_x} \delta_x a_{j+\delta_x}^\dagger a_j$. In the previous work [17], the conductivity is calculated through Fourier-transforming the current-current correlation numerically, whose time correlation is evaluated with use of the Suzuki-Trotter-decomposition approximation. We evaluate the resolvent form of equation (14) directly,

$$\sigma(\omega) = {\rm Re} \left(\frac{\rm i}{\hbar\omega {\rm L}^2} \times \left[\left\langle J_x \left(\frac{\hbar}{E_{\rm g} - \mathcal{H} + \hbar\omega} + \frac{\hbar}{E_{\rm g} - \mathcal{H} - \hbar\omega} \right) J_x \right\rangle \right]_{\rm av} \right). \qquad (15)$$

Now, we are free from the discrete numerical integration error. (The conductivity is a linear combination of the delta-function peaks as is apparent from Eq. (15), which might be suffered significantly from the numerical discretization error.) Some might wonder that the inverse matrix of the total Hamiltonian in equation (15) cannot be computed; this is true. The *expectation value* of the inverse of the Hamiltonian is, however, evaluated with use of the Gagliano-Balseiro continued-fraction formula [23],

$$\left\langle f_0 \left| \frac{1}{z - \mathcal{H}} \right| f_0 \right\rangle = \cfrac{\langle f_0 | f_0 \rangle}{z - \alpha_0 - \cfrac{\beta_1^2}{z - \alpha_1 - \cfrac{\beta_2^2}{\ddots}}}, \qquad (16)$$

where the coefficients are given by the Lanczos tridiagonal elements,

$$\begin{aligned} |f_{i+1}\rangle &= \mathcal{H}|f_i\rangle - \alpha_i |f_i\rangle - \beta_i^2 |f_{i-1}\rangle, \qquad (17) \\ \alpha_i &= \langle f_i | \mathcal{H} | f_i \rangle / \langle f_i | f_i \rangle, \\ \beta_i^2 &= \langle f_i | f_i \rangle / \langle f_{i-1} | f_{i-1} \rangle \quad (\beta_0 = 0). \end{aligned}$$

We have evaluated the dynamical conductivity (15) by means of this formula.

In Figure 5, we show the conductivity for a certain random sample with $\Delta = 1.25$ and $L = 5$. We see that the conductivity consists of delta-function peaks. The delta function peak is broadened into the Lorentz form through the substitution $\omega \to \omega - 0.2{\rm i}$. The concept of the dissipation becomes subtle for finite-size system. For instance, the DC conductivity is vanishing. This is due to the presence of the finite-size energy gap above the ground state. Only in the thermodynamic limit, The conductivity in the vicinity of the zero frequency $\omega = 0$ would emerge. (In the

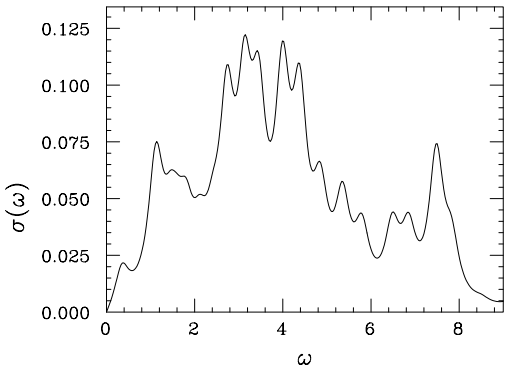

Fig. 5. Electrical conductivity is evaluated for a random sample with $\Delta = 1.25$ and $L = 5$. We see that the conductivity consists of delta-function peaks; the delta-function is broadened into the Lorentz form with the width $\eta = 0.2$.

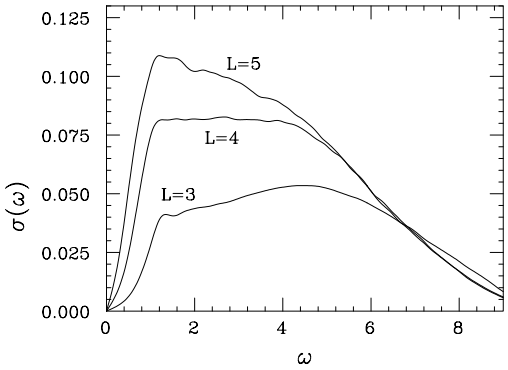

Fig. 6. Electrical AC conductivity is evaluated with the Gagliano-Balseiro formula (16) for $\Delta = 1.25$; the random-sample numbers are 16384, 2048 and 960 for $L = 3$, 4 and 5, respectively.

quantum Monte-Carlo simulation, the (real-)time correlation cannot be computed; the temperature (imaginary time) correlation function is computed instead. The latter is free from the delta-function singularities, because the poles exist only along the real-frequency axis. An analytical continuation to the real frequency, however, should be performed in order to estimate the dynamical response function such as equation (14). This is extremely difficult.)

In Figure 6, we show the random-averaged conductivity for $\Delta = 1.25$; the random-sample numbers are 16384, 2048 and 960 for $L = 3$, 4 and 5, respectively. We see that the conductivity increases as the frequency is reduced. In the vicinity of the static point $\omega \sim 0$, however, the conductivity drops rapidly due to the reason mentioned above (finite-size effect). (For comparison, we show the Fourier-transformed results [17]; $\sigma \approx 0.055$ for $L = 3$ and $\sigma \approx 0.105$ for $L = 4$. These are a bit larger than ours.) We estimate the DC conductivity as the maximal value of the AC conductivity. The DC conductivity shows large

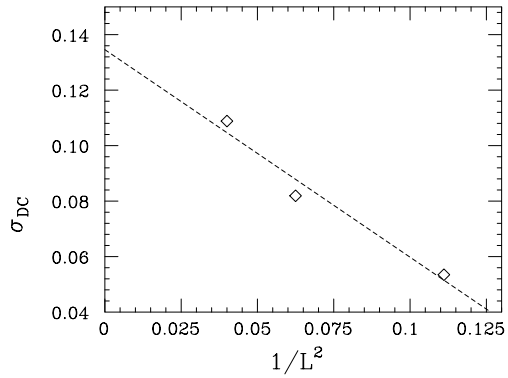

Fig. 7. $1/L^2$ extrapolation of the DC conductivity.

system-size dependence. In Figure 7, we depict the $1/L^2$ extrapolation of the conductivity. (The power 2 is chosen for the same reasoning as that in the paper [17].) The plots align. We stress that the present new data for $L = 5$ is crucial to confirm the validity of the $1/L^2$ extrapolation. We obtained the extrapolated conductivity with the least-square fit as $\sigma_c = 0.135 \pm 0.01((2e)^2/h)$.

3.3 Dynamical critical exponent

According to the conjecture introduced in Section 2.2, the dynamical critical exponent is given by $z = 2$ at the superfluid-localization transition. This conjecture has been confirmed numerically [17,20,22] with the help of the generalized Josephson relation (8) for the superfluid density. In fact, we demonstrated in Section 3.1 that the superfluid density is well described in terms of the generalized Josephson relation and the assumption $z = 2$. In this subsection, we utilize the Rieger-Young formula [24] for the first time in order to estimate z. We think that the scheme is suitable for the exact-diagonalization simulation, and gives z straightforwardly.

In Figure 8, we show the probability distribution of the first energy gap ΔE; $\Delta = 1.25$, $L = 5$ and 960 random samples. According to the Rieger-Young argument, from the low-energy tail of the distribution, the dynamical critical exponent is extracted: the probability of a certain energy gap may be proportional to the spatial volume $P \propto L^d \Delta E^\lambda$, where the exponent λ describes the low-energy tail. On the other hand, the finite-size scaling theory states that any quantities should be expressed in the form $P = \tilde{P}(L/\xi_r) = \tilde{P}(L/\xi_\tau^{1/z})$; see Section 2.2. With use of the formula $\Delta E \sim 1/\xi_\tau$, the distribution turns out to be a function of $L(\Delta E)^{1/z}$. Through collating this fact with the above form, we obtain the relation $\lambda = d/z$, which is the Rieger-Young relation.

In Figure 8, we see that the low-energy tail is, in fact, well described by the exponent $\lambda = 1$; namely, we obtain the estimate $z = d = 2$.

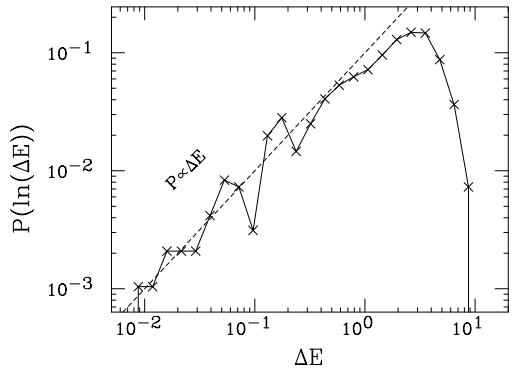

Fig. 8. Probability distribution of the first energy gap for the system with $\Delta = 1.25$ and $L = 5$.

4 Summary and discussions

We have investigated the two-dimensional hard-core boson system in the presence of the random chemical potential, whose Hamiltonian is given by (1). We diagonalized the Hamiltonian numerically for the system sizes up to $L = 5$. The present new data for $L = 5$ show no unexpected (irregular) behavior in the finite-size-scaling analysis. That is, the system sizes treated here reach scaling regime. This was not so certain, and in fact worried about in the previous study. We observed that the disorder-driven superfluid-localization transition takes place at the critical randomness $\Delta_c = 1.25 \pm 0.1$. We estimated the correlation-length exponent and the dynamical critical exponent as $\nu = 2.3 \pm 0.6$ and $z = 2$, respectively, with the finite-size scaling analysis. By means of the Gagliano-Balseiro method, we computed the dynamical conductivity at the critical point. Thereby, we obtained the DC conductivity $\sigma_c = 0.135 \pm 0.01((2e)^2/h)$.

Our estimate of the critical point is accordant with that of Runge [17]: by means of the same numerical method as ours, Runge obtained $\Delta_c \sim 1.15$ through the analysis of ρ_s, $\Delta_c \sim 1.25$ through the Binder parameter (the same as ours) and $\Delta_c \sim 1.1$–1.3 through $\langle \mathbf{m}_{XY}^2 \rangle$. The present new simulation for larger system size ($L = 5$) confirmed that the system size is surely in the scaling regime. On the other hand, by means of the quantum Monte-Carlo method it has been reported that the transition point locates at $\Delta_c = 1.43 \pm 0.06$ [22] and 0.72 [18] (in our definition). These estimates are based on the generalized Josephson relation (8) and an assumption of z; the former assumed $z = 2$, whereas the latter assumed $z = 0.5$. We think that the Binder parameter of the gauge order (12), which is readily computed with the exact-diagonalization scheme, shows less correction to the finite-size scaling.

Secondly, we discuss the correlation-length exponent ν. It should be made clear why our estimate $\nu = 2.3 \pm 0.6$ differs from that of reference [17] ($\nu = 1.4 \pm 0.3$) despite of the fact that we considered the same model by means of the same numerical technique except for our extension to $L = 5$. Crucial difference might be the criteria utilized to appreciate the data collapse in the scaling analysis. As is explained in Appendix, we used a quantitative scheme which also gives the estimate of the error margin. The error margin is, however, determined through taking account of only the statistical error, but not the correction to finite-size scaling. The latter is hardly appreciable quantitatively. Hence, there is a possibility that the error margin would be somewhat larger. The estimate of reference [17] lies a bit outside of our error bar, and, in fact, the scaling plot based on the assumption $\nu = 1.4$ does not show distinct failure as far as one can see. We believe, however, that our quantitative criterion would be objective and possibly less biased, although the present error margin might be rather large. At least, our data shown in Figure 9 seem to exclude the conclusion $\nu \sim 1$. In fact, Chayes *et al.* claimed an inequality $\nu \geq 2/d$, [30,31] which casts doubt on $\nu < 1$.

Next, we turn to discuss the dynamical critical exponent. We have used the Rieger-Young relation for the first time to estimate the dynamical critical exponent. The analysis showed a clear evidence that $z\,(= d) = 2$ holds. Because the previous estimates founded on the generalized Josephson relation (8) indicate the same conclusion as well, we believe that the prediction $z = d$ is established fairly definitely in two dimensions.

Finally, we mention about the electrical conductivity. The present conclusion $\sigma_c/((2e)^2/h) = 0.135 \pm 0.01$ is comparable with the estimates 0.17 ± 0.01 [17] and 0.14 ± 0.03 [20]. We stress that the previous exact-diagonalization data [17] for $L = 3$ and 4 are rather far from convergence, and our result for $L = 5$ reveled that the result of the system size is about to converge to a certain thermodynamic-limit value. In fact, as is shown in Figure 7, our new data $L = 5$ is vital in order to confirm the validity of the $1/L^2$ extrapolation. Quantum Monte-Carlo method is less efficient in computing dynamical quantity. (In the quantum Monte-Carlo simulation, the temperature (imaginary time) correlation rather than the time correlation is evaluated instead. The temperature correlation is fitted by an analytical function so as to yield the time correlation through the Wick rotation.) The present calculation with the help of the Gagliano-Balseiro method compensates the disadvantage.

In the paper [32,33], the authors claim that the limit $\omega \to 0$ at $T = 0$, which is used in the present paper, fails to give the DC conductivity relevant to the experimental transport measurements. According to their theory, the AC conductivity shows a Drude-like peak with the width $k_B T/\hbar$. Hence, at $T \to 0$, the peak vanishes to a single point so as to make the AC conductivity singular (discontinuous) at $\omega = 0$. Through taking account of this, the authors succeeded in explaining the experimentally observed critical conductivity $\approx (2e)^2/h$. Our numerical simulation is rather incapable of observing the features they proposed. This remained to be solved in future.

Our program is based on the subroutine package TITPACK ver. 2 coded by professor H. Nishimori. Numerical simulations were performed on VPP/700 56 of the computer center,

Kyushu university and VPP/500 of the Supercomputer Center, Institute for Solid State Physics, University of Tokyo.

Appendix: Details of the present scaling analyses

We explain the details of our finite-size-scaling analyses, which we managed in Section 3 in order to estimate the transition point Δ_c and the exponent ν. We adjusted these scaling parameters so that the scaled data shown in Figure 3 form a universal curve irrespective of the system sizes. In order to see quantitatively to what extent these data align, we employ the "local linearity function" S defined by Kawashima and Ito [29]: suppose a set of the data points $\{(x_i, y_i)\}$ with the error-bar $\{d_i(=\delta y_i)\}$, which we number so that $x_i < x_{i+1}$ may hold for $i = 1, 2, \cdots, n-1$. For this data set, the local-linearity function is defined as

$$S = \sum_{i=2}^{n-1} w(x_i, y_i, d_i | x_{i-1}, y_{i-1}, d_{i-1}, x_{i+1}, y_{i+1}, d_{i+1}). \tag{A.1}$$

The quantity $w(x_j, y_j, d_j | x_i, y_i, d_i, x_k, y_k, d_k)$ is given by

$$w = \left(\frac{y_j - \bar{y}}{\Delta}\right)^2 , \tag{A.2}$$

where

$$\bar{y} = \frac{(x_k - x_j)y_i - (x_i - x_j)y_k}{x_k - x_i} \tag{A.3}$$

and

$$\Delta^2 = d_j^2 + \left(\frac{x_k - x_j}{x_k - x_i} d_i\right)^2 + \left(\frac{x_i - x_j}{x_k - x_i} d_k\right)^2 . \tag{A.4}$$

In other words, the numerator $y_j - \bar{y}$ denotes the deviation of the point (x_j, y_j) from the line passing two points (x_i, y_i) and (x_k, y_k), and the denominator Δ stands for the statistical error of $(y_i - \bar{y})$. And so, $w = ((y_i - \bar{y})/\Delta)^2$ shows a degree to what extent these three points align. The advantage in the above analysis is as follows: in the conventional least square fitting, we need to assume some particular fitting function. The assumption which function we use causes systematic error. Note that in the present analysis, we do not have to assume any fitting functions.

The scaling parameters are determined so as to minimize the local-linearity function. The error margin of the scaling parameter is hard to estimate. It is concerned with both the statistical error and the correction to the finite size scaling. The former error can be estimated through considering the statistical error of the function S. This function has a relative error of the order $1/\sqrt{n-2}$. (The local-linearity function is of the order $(n-2)$, and the error is given by $\sqrt{n-2}$.) The correction to the finite-size scaling, on the contrary, is quite difficult to determine. Here, we consider only the statistical error in order to estimate the error margins of the scaling parameters. As the number of the data points n is increased, the statistical error of S is reduced. The corrections to the finite-size scaling might increase instead. In the present analyses, we used twenty data in the vicinity of the transition point Δ_c. An example of the plot S is shown in Figure 9. We observe the minimum at $\nu = 2.0$. Taking into account of the statistical error, we estimated the critical exponent as $\nu = 2.3 \pm 0.6$.

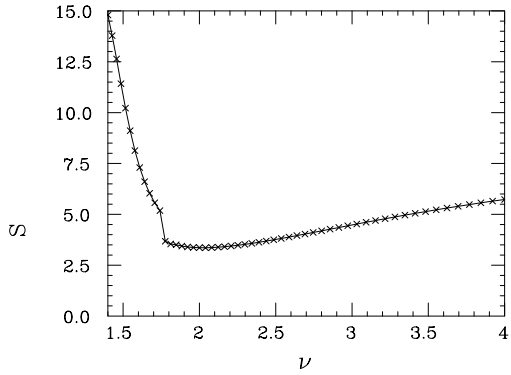

Fig. 9. Local linearity function is plotted with varying the scaling parameter ν. From this plot, we estimated the exponent as $\nu = 2.3 \pm 0.6$.

References

1. E. Abrahams, P.W. Anderson, D.C. Licciardello, T.V. Ramakrishnan, Phys. Rev. Lett. **42**, 673 (1979).
2. D.B. Haviland, Y. Liu, A.M. Goldman, Phys. Rev. Lett **62**, 2180 (1989).
3. Y. Liu, K.A. McGreer, B. Nease, D.B. Haviland, G. Marinez, J.W. Halley, A.M. Goldman, Phys. Rev. Lett. **67**, 2068 (1991).
4. S.J. Lee, J.B. Ketterson, Phys. Rev. Lett. **64**, 3078 (1990).
5. A.F. Hebard, M.A. Paalanen, Phys. Rev. Lett. **54**, 2155 (1985).
6. T. Wang, K.M. Beauchamp, D.D. Berkley, B.R. Johnson, J.-X. Liu, J. Zhang, A.M. Goldman, Phys. Rev. B **43**, 8623 (1991).
7. L.J. Geerligs, M. Peters, L.E.M. de Groot, A. Verbruggen, J.E. Mooji, Phys. Rev. Lett. **63**, 326 (1989).
8. S. Katsumoto, J. Low Temp. Phys. **98**, 287 (1995).
9. B.C. Crooker, B. Hebral, E.N. Smith, Y. Takano, J.D. Reppy, Phys. Rev. Lett. **22**, 666 (1983).
10. D. Finotello, K.A. Gillis, A. Wong, M.H. Chan, Phys. Rev. Lett. **61**, 1954 (1988).
11. M. Ma, B.I. Halperin, P.A. Lee, Phys. Rev. B **34**, 3136 (1986).
12. M.P.A. Fisher, P.B. Weichman, G. Grinstein, D.S. Fisher, Phys. Rev. B. **40**, 546 (1989).
13. T. Giamarch, H.J. Schulz, Europhys. Lett. **3**, 1287 (1987).
14. M.P.A. Fisher, G. Grinstein, S.M. Girvin, Phys. Rev. Lett. **64**, 587 (1990).
15. A.C. Doty, D.S. Fisher, Phys. Rev. B **45**, 2167 (1992).
16. N. Hatano, J. Phys. Soc. Jpn **64**, 1529 (1995).
17. K.J. Runge, Phys. Rev. B **45**, 13136 (1992).

18. M. Makivić, N. Trivedi, S. Ullah, Phys. Rev. Lett. **71**, 2307 (1993).
19. G.G. Batrouni, B. Larson, R.T. Scalettar, J. Tobochnik, J. Wang, Phys. Rev. B **48**, 9628 (1993).
20. M. Wallin, E.S. Sørensen, S.M. Girvin, A.P. Young, Phys. Rev. B **49**, 12115 (1994).
21. E.S. Sørensen, M. Wallin, S.M. Girvin, A.P. Young, Phys. Rev. Lett. **69**, 828 (1992).
22. S. Zhang, N. Kawashima, J. Carlson, J.E. Gubernatis, Phys. Rev. Lett. **74**, 1500 (1995).
23. E.R. Gagliano, C.A. Balseiro, Phys. Rev. Lett. **59**, 2999 (1987).
24. H. Rieger, A.P. Young, Phys. Rev. B **54**, 3328 (1996).
25. T. Matsubara, H. Matsuda, Prog. Theor. Phys. **16**, 569 (1956).
26. T. Kishi, K. Kubo, J. Phys. Soc. Jpn **58**, 2547 (1989).
27. M.E. Fisher, M.N. Barber, D. Jasnow, Phys. Rev. A **8**, 1111 (1973).
28. K. Binder, Phys. Rev. Lett. **47**, 693 (1981).
29. N. Kawashima, N. Ito, J. Phys. Soc. Jpn **62**, 435 (1993).
30. J.T. Chayes, L. Chayes, D.S. Fisher, T. Spencer, Phys. Rev. Lett. **57**, 2999 (1986).
31. J.T. Chayes, L. Chayes, D.S. Fisher, T. Spencer, Commun. Math. Phys. **120**, 501 (1989).
32. K. Damle, S. Sachdev, Phys. Rev. B **56**, 8714 (1997).
33. I.F. Herbut, Phys. Rev. Lett. **81**, 3916 (1998).